Physics-Informed Online Learning of Flux Linkage Model for Synchronous Machines

1st Seunghun Jang, 2nd Myeongseok Ryu and 3rd Kyunghwan Choi
Cho Chun Shik Graduate School of Mobility
Korea Advanced Institute of Science and Technology
Daejeon, Republic of Korea
{shjang7071, dding_98 and kh.choi}@kaist.ac.kr

***Abstract*—The stator flux linkages serve as a key to the optimal control of synchronous machines (SMs). However, due to their complex and nonlinear characteristics, accurately modeling and identifying them online remains highly challenging. In this regard, neural network-based learning strategies are considered promising candidates for modeling the flux linkages, but their application has so far been largely limited to offline training of neural networks. Therefore, this study presents a physics-informed online learning method for accurately modeling the flux linkages of SMs. The proposed method enables online training of a neural network to learn the physical laws governing the flux linkages while adhering to the model's inherent physical constraints. The learning rules for updating the neural network weights are formulated to satisfy the first-order optimality conditions, and the proposed method can be employed as an online flux linkage estimator. The effectiveness of the proposed method is validated through simulation results conducted on a 35 kW interior permanent magnet synchronous machine (IPMSM) drive.**

***Index Terms*—Physics-informed learning, stator flux linkages, synchronous machines (SMs), online identification**

I. Introduction

A. Motivation

The dynamic behavior of synchronous machines (SMs) is described by ordinary differential equations (ODEs) representing the time derivatives of the stator flux linkages [1]. Therefore, accurately obtaining the stator flux linkages is essential for achieving the optimal control of SMs, enabling advanced current control [2], optimal feedforward control [3], and optimization-based methods such as generalized model predictive torque control (GMPTC) [4].

A straightforward approach to identifying the stator flux linkages in SMs is to construct flux linkage maps through experimental identification techniques, which are conducted offline under steady-state conditions across the entire operating range [5]. However, this strategy has several limitations: the experimental identification process is both time-consuming and costly, and the resulting maps cannot adapt to parameter variations arising from abnormal conditions such as temperature rise or demagnetization, as well as aging effects [6]. Therefore, online estimation of the stator flux linkage is desirable for accurate modeling of SMs.

*This work was supported by the National Research Foundation of Korea (NRF) grant funded by the Korea government (MSIT) (RS-2025-00554087). (*Corresponding author: Kyunghwan Choi*)

B. Literature Review

Several studies have proposed online estimation approaches for stator flux linkages. In [7], flux linkages are estimated by integrating the voltage model (ODEs describing the SM in the α-β reference frame) and compensating for DC offset errors using a high-pass filter, but this approach distorts the low-frequency response. Furthermore, [8] proposes a Gopinath-style observer combining the voltage and current flux models without considering cross-coupling effects, whereas [9] compensates for these effects only under steady-state conditions by using the integrator errors of the current controllers.

Recently, state observer-based estimators have shown remarkable estimation performance. The disturbance observer-based flux linkage estimator (DOBFLE) in [10] and the extended state observer-based flux linkage estimator (ESOFLE) in [11] decompose the flux linkage into linear and nonlinear components, and estimate them separately. [12] proposed a linear state observer that estimates the integration errors arising from integrating the voltage model of SMs, and directly compensates for them based on the integration results. These approaches guarantee exponential convergence in steady state even when nominal parameters (i.e., nominal inductances) are used; however, if the parameters used in observer design deviate considerably from their actual values, the transient estimation performance may deteriorate.

Alternatively, data-driven approaches using neural networks (NN) show promise for learning nonlinear flux linkage models. In [13], a radial basis function (RBF)-based NN was utilized to learn the flux linkage model based on suboptimal solutions valid only under steady-state conditions of SM dynamics. [14] applied a multilayer perceptron (MLP) network to the dynamics of SM in discrete time, and updated the weight parameters online to learn the flux linkages and stator resistance; however, the study did not provide sufficient guarantees for the accuracy of flux linkage learning and requires a high-performance processor to implement the weight update optimization algorithm.

C. Contributions

The literature review confirms the limitations of existing approaches. To overcome the aforementioned challenges, this study proposes a neural network (NN)-based online learning approach for estimating the stator flux linkages. The key idea

is to model the stator flux linkages using a neural network and approximate them through physics-informed online learning via constrained optimization, thereby satisfying the first-order optimality conditions [15]. The contributions of the proposed method are as follows:

- The flux linkage model is represented by the NN and identified online via physics-informed learning , where the NN serves as the solution that satisfies the underlying physical laws [16]. To facilitate this learning, the electrical dynamics of SMs, originally expressed as ODEs, are reformulated into partial differential equations (PDEs).
- The physics-informed online learning process is formulated as a constrained optimization problem, which allows physical constraints to be imposed on the flux linkage during the learning process. This ensures accurate identification of the flux linkage model while simultaneously learning its behavior.
- The learning rules, derived from solving the constrained optimization problem, satisfy the first-order optimality conditions at steady states.

II. PRELIMINARIES

A. SM Model

The electrical dynamics of SM in the d-q reference frame is expressed as the following ODEs:

$$\frac{\mathrm{d}\psi_s^d(i_s^d, i_s^q)}{\mathrm{d}t} = -R_s i_s^d + w_r \psi_s^q(i_s^d, i_s^q) + v_s^d, \tag{1a}$$

$$\frac{\mathrm{d}\psi_s^q(i_s^d, i_s^q)}{\mathrm{d}t} = -R_s i_s^q - w_r \psi_s^d(i_s^d, i_s^q) + v_s^q, \tag{1b}$$

where ψ_s^d and ψ_s^q represent the d- and q-axis stator flux linkages, respectively; i_s^d and i_s^q, and v_s^d and v_s^q represent the stator currents and voltages corresponding to the d- and q-axes, respectively; R_s denotes the stator resistance; w_r represents the electrical rotor speed.

In this study, the following assumptions are considered for the above ODEs:

- The stator currents (i_s^d and i_s^q) and the electrical rotor speed (w_r) are accurately measurable.
- The stator resistance (R_s) is regarded as known.
- The inverter nonlinearities and the iron losses (resulting from eddy currents and hysteresis effects) are assumed to be negligible.

B. Interpreting ODEs in a PDE Framework

The stator flux linkages are generally modeled as nonlinear functions of the stator currents (i.e., $\psi_s^d(i_s^d, i_s^q)$ and $\psi_s^q(i_s^d, i_s^q)$). Using the chain rule with respect to stator currents i_s^d and i_s^q, the time derivatives of the flux linkages are given by

$$\frac{\mathrm{d}\psi_s^d(i_s^d, i_s^q)}{\mathrm{d}t} = \underbrace{\frac{\partial \psi_s^d}{\partial i_s^d}}_{=:L_s^{dd}} \frac{\mathrm{d}i_s^d}{\mathrm{d}t} + \underbrace{\frac{\partial \psi_s^d}{\partial i_s^q}}_{=:L_s^{dq}} \frac{\mathrm{d}i_s^q}{\mathrm{d}t}, \tag{2a}$$

$$\frac{\mathrm{d}\psi_s^q(i_s^d, i_s^q)}{\mathrm{d}t} = \underbrace{\frac{\partial \psi_s^q}{\partial i_s^d}}_{=:L_s^{qd}} \frac{\mathrm{d}i_s^d}{\mathrm{d}t} + \underbrace{\frac{\partial \psi_s^q}{\partial i_s^q}}_{=:L_s^{qq}} \frac{\mathrm{d}i_s^q}{\mathrm{d}t}, \tag{2b}$$

where the partial derivatives are defined as the differential inductances: L_s^{dd} and L_s^{qq} denote the d- and q-axis self-differential inductances, respectively, while L_s^{dq} and L_s^{qd} represent the corresponding mutual differential inductances [2].

Consequently, by substituting (2a) and (2b) into (1a) and (1b), respectively, the ODEs (1) can be reformulated as the following PDEs

$$\frac{\partial \psi_s^d}{\partial i_s^d}\frac{\mathrm{d}i_s^d}{\mathrm{d}t} + \frac{\partial \psi_s^d}{\partial i_s^q}\frac{\mathrm{d}i_s^q}{\mathrm{d}t} = -R_s i_s^d + w_r \psi_s^q(i_s^d, i_s^q) + v_s^d, \tag{3a}$$

$$\frac{\partial \psi_s^q}{\partial i_s^d}\frac{\mathrm{d}i_s^d}{\mathrm{d}t} + \frac{\partial \psi_s^q}{\partial i_s^q}\frac{\mathrm{d}i_s^q}{\mathrm{d}t} = -R_s i_s^q - w_r \psi_s^d(i_s^d, i_s^q) + v_s^q, \tag{3b}$$

which are employed as governing equations for the physics-informed online learning of the flux linkage model (see Section III-A for more details).

C. Physical Constraints on Flux Linkage

According to the principle of magnetic energy conservation for all admissible stator currents, the self-differential inductances must always be positive [2]. More specifically, the bounds of these inductances are determined by the physical properties of SMs, e.g.,

$$\begin{aligned} \underline{L}_{\mathrm{s}}^{dd} < L_s^{dd}(i_s^d, i_s^q) < \overline{L}_{\mathrm{s}}^{dd}, \\ \underline{L}_{\mathrm{s}}^{qq} < L_s^{qq}(i_s^d, i_s^q) < \overline{L}_{\mathrm{s}}^{qq}, \end{aligned} \tag{4}$$

where $\underline{L}_{\mathrm{s}}^{dd}$ and $\underline{L}_{\mathrm{s}}^{qq}$, and $\overline{L}_{\mathrm{s}}^{dd}$ and $\overline{L}_{\mathrm{s}}^{qq}$ represent the lower and upper bounds of the self-differential inductances, respectively.

III. PHYSICS-INFORMED ONLINE LEARNING OF FLUX LINKAGE MODEL

This section presents a physics-informed online learning method for approximating the solution of the PDEs (3) using a neural network (NN). First, the NN architecture for online learning is introduced in Section III-A, and a constrained optimization problem for NN learning is formulated in Section III-B. Subsequently, this optimization problem is solved in Section III-C using the proposed learning rules, yielding solutions that satisfy the Karush-Kuhn-Tucker (KKT) conditions (i.e., the first-order optimality conditions).

A. NN Architecture

For online learning, a typical three-layer NN structure (i.e., input layer, hidden layer, and output layer with weights) is employed as the neural network architecture, which can approximate the nonlinear behavior between the stator flux linkages (ψ_s^d and ψ_s^q) and the stator currents (i_s^d and i_s^q). Invoking this relationship leads to the following expressions:

$$\psi_s^d(i_s^d, i_s^q) = \boldsymbol{w}_d^\top \boldsymbol{\sigma}_d(\boldsymbol{x}) + \epsilon_{\mathrm{s}}^d, \tag{5a}$$

$$\psi_s^q(i_s^d, i_s^q) = \boldsymbol{w}_q^\top \boldsymbol{\sigma}_q(\boldsymbol{x}) + \epsilon_{\mathrm{s}}^q, \tag{5b}$$

where $\boldsymbol{x} := \left(i_s^d, i_s^q\right)^\top \in \mathbb{R}^2$ denotes the input vector; $\boldsymbol{w}_d \in \mathbb{R}^n$ and $\boldsymbol{w}_q \in \mathbb{R}^m$ represent the d- and q-axis weight vectors, respectively; $\boldsymbol{\sigma}_d \in \mathbb{R}^n$ and $\boldsymbol{\sigma}_q \in \mathbb{R}^m$ are the nonlinear activation functions for the d- and q-axes; and ϵ_{s}^d and ϵ_{s}^q are the approximation errors bounded by sufficiently small positive

values. Accordingly, the data-driven approximation of the flux linkages is expressed as

$$\hat{\psi}_s^d(\hat{\boldsymbol{w}}_d, \boldsymbol{x}) = \hat{\boldsymbol{w}}_d^\top \boldsymbol{\sigma}_d(\boldsymbol{x}), \tag{6a}$$
$$\hat{\psi}_s^q(\hat{\boldsymbol{w}}_q, \boldsymbol{x}) = \hat{\boldsymbol{w}}_q^\top \boldsymbol{\sigma}_q(\boldsymbol{x}), \tag{6b}$$

where $\hat{\boldsymbol{w}}_d \in \mathbb{R}^n$ and $\hat{\boldsymbol{w}}_q \in \mathbb{R}^m$ are the estimated output layer weight vectors for the d- and q-axis flux linkages, respectively, which are updated online.

In a compact space, if the true flux linkage in (5) is at least piecewise continuous, activation functions such as sigmoid and hyperbolic tangent functions have universal approximation properties almost everywhere (except on a set of measure zero) [17]. The number of these activation functions acts as a hyperparameter tuned by a designer. Therefore, to construct the optimal learning model, the ideal functions proposed in [18], which inherently represent the behavior of the flux linkages, are utilized as activation functions, e.g.,

$$\boldsymbol{\sigma}_d(\boldsymbol{x}) = \left(a_0,\, a_1 i_s^d,\, a_2 (i_s^d)^2,\, a_3 i_s^q,\, a_4 \tanh\left(i_s^d\right)\right)^\top, \tag{7a}$$
$$\boldsymbol{\sigma}_q(\boldsymbol{x}) = \left(b_0,\, b_1 i_s^q,\, b_2 (i_s^q)^2,\, b_3 i_s^d,\, b_4 \tanh\left(i_s^q\right)\right)^\top, \tag{7b}$$

where $a_0, \ldots, a_4$ and $b_0, \ldots, b_4$ are the design parameters.

Training the NN is generally performed by updating its weights through regression or backpropagation to minimize the error between the network's forward prediction and the actual outputs. However, it is challenging to directly use the flux linkages as outputs, as they cannot be measured in the absence of a flux sensor. Instead, the PDEs (3) can be utilized for NN learning by expressing them as residuals of the governing equations, and updating the network weights such that these residuals approach zero. The PDE residuals are expressed as follows:

$$e_{\mathrm{s}}^d := \hat{L}_s^{dd} \frac{\mathrm{d}i_s^d}{\mathrm{d}t} + \hat{L}_s^{dq} \frac{\mathrm{d}i_s^q}{\mathrm{d}t} + R_s i_s^d - w_r \hat{\psi}_s^q - v_s^d, \tag{8a}$$
$$e_{\mathrm{s}}^q := \hat{L}_s^{qd} \frac{\mathrm{d}i_s^d}{\mathrm{d}t} + \hat{L}_s^{qq} \frac{\mathrm{d}i_s^q}{\mathrm{d}t} + R_s i_s^q + w_r \hat{\psi}_s^d - v_s^q, \tag{8b}$$

with the estimated (denoted by $\hat{}$) differential inductances

$$\hat{L}_s^{dd}(\hat{\boldsymbol{w}}_d, \boldsymbol{x}) := \frac{\partial \hat{\psi}_s^d}{\partial i_s^d} = \hat{\boldsymbol{w}}_d^\top \frac{\partial \boldsymbol{\sigma}_d(\boldsymbol{x})}{\partial i_s^d}, \tag{9a}$$
$$\hat{L}_s^{dq}(\hat{\boldsymbol{w}}_d, \boldsymbol{x}) := \frac{\partial \hat{\psi}_s^d}{\partial i_s^q} = \hat{\boldsymbol{w}}_d^\top \frac{\partial \boldsymbol{\sigma}_d(\boldsymbol{x})}{\partial i_s^q}, \tag{9b}$$
$$\hat{L}_s^{qd}(\hat{\boldsymbol{w}}_q, \boldsymbol{x}) := \frac{\partial \hat{\psi}_s^q}{\partial i_s^d} = \hat{\boldsymbol{w}}_q^\top \frac{\partial \boldsymbol{\sigma}_q(\boldsymbol{x})}{\partial i_s^d}, \tag{9c}$$
$$\hat{L}_s^{qq}(\hat{\boldsymbol{w}}_q, \boldsymbol{x}) := \frac{\partial \hat{\psi}_s^q}{\partial i_s^q} = \hat{\boldsymbol{w}}_q^\top \frac{\partial \boldsymbol{\sigma}_q(\boldsymbol{x})}{\partial i_s^q}, \tag{9d}$$

which are obtained by analytically differentiating the activation functions in (7) with respect to the stator currents, and then substituting the results into (9).

In addition to the partial derivatives derived in (9), the evaluation of the PDE residuals (8) also requires the time derivatives of the stator currents. These time derivatives are approximated using the Euler method with a sampling time T_s as follows:

$$\frac{\mathrm{d}i_s^d}{\mathrm{d}t} \approx \frac{i_s^d[k] - i_s^d[k-1]}{T_s}, \quad \frac{\mathrm{d}i_s^q}{\mathrm{d}t} \approx \frac{i_s^q[k] - i_s^q[k-1]}{T_s},$$

where k denotes the current time step. Consequently, the resulting PDE residuals are utilized to update the output layer weights for learning the NN. The architecture of the proposed NN is illustrated in Fig. 1.

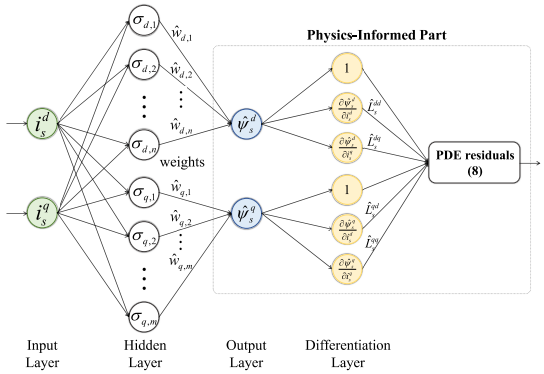

Fig. 1: The proposed NN architecture for the physics-informed online learning.

Remark 1. *This study focuses on approximating the solutions of the PDEs* (3) *by updating only the output layer weights of a single-hidden-layer neural network (i.e., linear-in-parameter structure). Owing to its simplicity, this structure is well suited for use as an online flux linkage estimator itself. However, the proposed method has the potential to be extended to multi-layer neural networks with nonlinear-in parameter structure, enabling online learning of the global behavior of the flux linkage using meaningful datasets collected under various operating conditions.*

B. Problem Formulation

Considering the physical constraints of SMs, the optimization problem is formulated as

$$\min_{\hat{\boldsymbol{w}}} J(\boldsymbol{e}; \hat{\boldsymbol{w}}) = \frac{1}{2} \boldsymbol{e}^\top \boldsymbol{e} \tag{10a}$$
subject to
$$c_1^{\mathrm{in}}(\hat{\boldsymbol{w}}) = \hat{L}_{\mathrm{s}}^{dd}(\hat{\boldsymbol{w}}_d, \boldsymbol{x}) - \overline{L}_{\mathrm{s}}^{dd} \leq 0, \tag{10b}$$
$$c_2^{\mathrm{in}}(\hat{\boldsymbol{w}}) = -\hat{L}_{\mathrm{s}}^{dd}(\hat{\boldsymbol{w}}_d, \boldsymbol{x}) + \underline{L}_{\mathrm{s}}^{dd} \leq 0, \tag{10c}$$
$$c_3^{\mathrm{in}}(\hat{\boldsymbol{w}}) = \hat{L}_{\mathrm{s}}^{qq}(\hat{\boldsymbol{w}}_q, \boldsymbol{x}) - \overline{L}_{\mathrm{s}}^{qq} \leq 0, \tag{10d}$$
$$c_4^{\mathrm{in}}(\hat{\boldsymbol{w}}) = -\hat{L}_{\mathrm{s}}^{qq}(\hat{\boldsymbol{w}}_q, \boldsymbol{x}) + \underline{L}_{\mathrm{s}}^{qq} \leq 0, \tag{10e}$$

where $J \in \mathbb{R}$ is the objective function, $\boldsymbol{e} := \left(e_{\mathrm{s}}^d, e_{\mathrm{s}}^q\right)^\top \in \mathbb{R}^2$ is the PDE residual vector, and $\hat{\boldsymbol{w}} := \left(\hat{\boldsymbol{w}}_d^\top, \hat{\boldsymbol{w}}_q^\top\right)^\top \in \mathbb{R}^{n+m}$ denotes the estimated weight vector, which is the optimization variable in (10). The objective function (10a) is employed to optimize the weights via simultaneous approximation of the flux linkages and inductances using the PDE residuals (8).

The inequality constraints ($c_j^{\text{in}} \leq 0,\ j \in \mathcal{I} = \{1,2,3,4\}$) in (10b)–(10e) are designed considering the physical properties of SMs, as discussed in Section II-C.

C. Learning Rules

The solutions to the constrained optimization problem (10) are obtained by satisfying the optimality conditions of the Lagrangian function, which is defined as follows:

$$\mathcal{L}(\boldsymbol{e}, \hat{\boldsymbol{w}}, \boldsymbol{\lambda}^{\text{in}}) := J(\boldsymbol{e}; \hat{\boldsymbol{w}}) + \sum_{j \in \mathcal{I}} \lambda_j^{\text{in}} c_j^{\text{in}}(\hat{\boldsymbol{w}}), \tag{11}$$

where $\lambda_j^{\text{in}} \in \mathbb{R},\ \forall j \in \mathcal{I}$ is the Lagrange multiplier for the inequality constraint c_j^{in}.

To solve the optimization problem, considering the Lagrangian function (11) with respect to two variables (i.e., $\hat{\boldsymbol{w}}$ and $\boldsymbol{\lambda}^{\text{in}}$), the problem can be reformulated as a primal-dual problem

$$\min_{\hat{\boldsymbol{w}}} \max_{\lambda_{j \in \mathcal{I}}^{\text{in}}} \mathcal{L}(\boldsymbol{e}, \hat{\boldsymbol{w}}, \boldsymbol{\lambda}^{\text{in}}). \tag{12}$$

The learning rules for satisfying the KKT optimality conditions of (12) are derived as

$$\dot{\hat{\boldsymbol{w}}} = -\alpha \frac{\partial \mathcal{L}(\boldsymbol{e}, \hat{\boldsymbol{w}}, \boldsymbol{\lambda}^{\text{in}})}{\partial \hat{\boldsymbol{w}}} = -\alpha \left(\frac{\partial J}{\partial \hat{\boldsymbol{w}}} + \sum_{j \in \mathcal{I}} \lambda_j^{\text{in}} \frac{\partial c_j^{\text{in}}}{\partial \hat{\boldsymbol{w}}} \right), \tag{13a}$$

$$\dot{\lambda}_j^{\text{in}} = \beta_j^{\text{in}} \frac{\partial \mathcal{L}(\boldsymbol{e}, \hat{\boldsymbol{w}}, \boldsymbol{\lambda}^{\text{in}})}{\partial \lambda_j} = \beta_j^{\text{in}} c_j^{\text{in}}(\hat{\boldsymbol{w}}), \quad \forall j \in \mathcal{I}, \tag{13b}$$

$$\lambda_j^{\text{in}} \leftarrow \max(\lambda_j^{\text{in}}, 0), \tag{13c}$$

where α and β_j^{in} denote the learning rates (positive constants) for the weight vectors and Lagrange multipliers, respectively.

Under the learning rules (13), when the inequality constraint c_j^{in} is inactive (i.e., $c_j^{\text{in}} < 0$), the Lagrange multiplier λ_j^{in} gradually decreases and converges to zero, while the weights are updated in the direction of gradient descent to minimize the Lagrangian function. If the inequality constraint becomes active (i.e., $c_j^{\text{in}} \geq 0$), λ_j^{in} increases until c_j^{in} reaches the equality boundary (i.e., $c_j^{\text{in}} = 0$), after which the update follows the same behavior as in the inactive case. At the stationary point, the KKT optimality conditions are satisfied, i.e., $\frac{\partial \mathcal{L}}{\partial \hat{\boldsymbol{w}}} = 0$, $c_j^{\text{in}} \leq 0$, $\lambda_j^{\text{in}} \geq 0$, and $\lambda_j^{\text{in}} c_j^{\text{in}} = 0$, where $\dot{\hat{\boldsymbol{w}}} \to 0$ and $\dot{\lambda}_j^{\text{in}} \to 0$ at steady state.

Remark 2. *The proposed learning rules* (13) *guarantee only the first-order necessary conditions for optimality; therefore, the solutions to the problem* (10) *may correspond to a local minimum, a local maximum, or a saddle point. However, even though the obtained solutions may be a local optimum, the enforcement of physical constraints guides the learning rules* (13) *to find improved solutions within the imposed constraints, thereby leading to enhanced performance compared to unconstrained approaches.*

TABLE I: Specifications for the IPMSM

Parameter	Value
Rated mech. power	35 kW
Rated mech. speed	2000 RPM
Rated mech. torque	180 Nm
Max. stator voltage (v_{s})	160 V
Max. stator current (i_{s})	350 A
Pole pairs (P)	8
Stator resistance (R_s)	10.7 mΩ

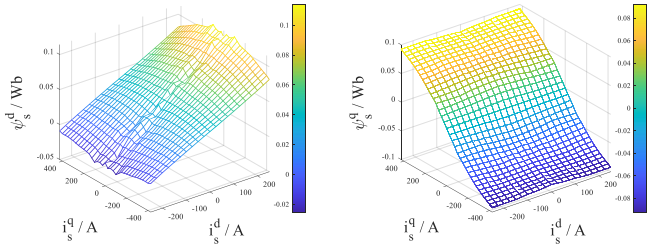

(a) (b)

Fig. 2: Stator flux linkage maps of the IPMSM corresponding to the d-axis (a) and q-axis (b).

IV. Simulation Validation

A. Simulation Setup

Simulation validation was conducted using MATLAB & Simulink R2024b to verify the feasibility of the proposed physics-informed online learning method. The simulation environment was adapted from the '`Three-phase PMSM Traction Drive`' example, incorporating the proposed method within the control framework. The specifications of the 35 kW IPMSM model used in this environment are listed in Table I, and the corresponding flux linkage maps, constructed using 2-D lookup tables (LUTs) for the differential inductances (L_s^{dd} and L_s^{qq}) and the permanent magnet flux linkage (ψ_{pm}), are shown in Fig. 2. The IPMSM drive was regulated according to a maximum torque per ampere (MTPA) trajectory obtained through the numerical algorithm described in [19], and subsequently, current references derived from the desired torque were tracked via a PI current controller with feedforward compensation.

The proposed method enables online learning of the flux linkage model and can be directly employed as a flux linkage estimator itself. For the comparison of flux estimation performance, the proposed method was compared with the true flux linkage model and the state-of-the-art disturbance observer-based flux linkage estimator (DOBFLE) [10] under torque reference variations between 0 and 180 Nm with a 50 Hz bandwidth at 500 RPM mechanical speed. The stator voltage used for flux estimation was generated by a current controller with a bandwidth of 200 Hz and a control sampling time $T_s = 50\ \mu$s. The simulation settings for this comparative study are described in detail as follows:

1) *Actual Flux Linkage Model:* A 2-D data model based on LUTs extracted from the FEM-parameterized IPMSM was used as the reference model.

2) *DOBFLE:* This method separates the flux linkage into linear terms and nonlinear disturbance terms, defines them as state variables, and designs a state observer to estimate these states (see [10] for details). The observer gain matrix $\boldsymbol{F}$, associated with the state observer, was designed by formulating a linear matrix inequality (LMI) problem to place the eigenvalues of the observer's closed-loop system at a bandwidth of 100 Hz (i.e., 628 rad/s), using the nominal inductance matrix $\boldsymbol{L}_{\mathrm{s},0} = \begin{bmatrix} 0.25 & 0 \\ 0 & 0.32 \end{bmatrix}$ mH. The problem was solved using YALMIP with the MOSEK solver, and the resulting gain matrix was given by $\boldsymbol{F} = \begin{bmatrix} 0.1377 & 0.4688 & -0.1609 & 0.4644 \\ -0.5726 & 0.1703 & -0.5672 & -0.1965 \end{bmatrix}^{\top}$.

3) *Proposed Method (PM):* For learning the NN, the number of neurons used in the activation functions was configured as $n = 5$ and $m = 5$, and the parameters in (7) were set to $a_0 = 120$, $a_1 = 1$, $a_2 = 6.9 \cdot 10^{-6}$, $a_3 = 2.6 \cdot 10^{-3}$, $a_4 = 1$, and $b_0 = 0.5$, $b_1 = 1$, $b_2 = 6.9 \cdot 10^{-6}$, $b_3 = 2.6 \cdot 10^{-3}$, $b_4 = 1$. The weights were updated with the sampling time T_s, and the learning rates for the weights and the Lagrange multipliers were set as $\alpha = 50$ and $\beta^{\mathrm{in}}_{j\in\mathcal{I}} = 1.5 \cdot 10^{6}$, respectively. The upper and lower bounds for L_s^{dd} and L_s^{qq} were selected as $\overline{L}_{\mathrm{s}}^{dd} = 3.0 \cdot 10^{-4}$, $\underline{L}_{\mathrm{s}}^{dd} = 2.5 \cdot 10^{-4}$, $\overline{L}_{\mathrm{s}}^{qq} = 4.5 \cdot 10^{-4}$, and $\underline{L}_{\mathrm{s}}^{qq} = 2.5 \cdot 10^{-4}$, respectively.

B. Simulation Results

Figure 3 shows the simulation results of the stator flux linkage estimates under varying torque command. As shown in Fig. 3a, the flux estimation performance of the PM was compared with that of the actual flux linkage model and the DOBFLE. In Fig. 3b, the self differential inductance estimates are shown with the Lagrange multipliers representing the corresponding constraints.

During the identification sequence in Fig. 3a, the torque command $T_{\mathrm{e}}^{\mathrm{cmd}}$ increased to 180 Nm with step signals from $t = 0.05$ s to $t = 0.25$ s, and then decreased to 0 Nm at $t = 0.55$ s. In this scenario, the d-axis flux linkage ψ_s^d varied from 0.018 Wb to 0.044 Wb, while the q-axis flux linkage ψ_s^q changed from 0.0 Wb to 0.08 Wb. Both the PM and the DOBFLE exhibited flux linkage estimation errors that converged to near zero in steady states within the bandwidth of the torque reference (i.e., 50 Hz). However, in the DOBFLE, the observer gain matrix was designed based on nominal inductance parameters, which could not account for changes in inductance under varying torque conditions. As a result, estimation errors occurred throughout the transient states due to the deviation between the nominal and actual inductances, with particularly large errors observed in the d-axis flux linkage from $t = 0.05$ s to $t = 0.07$ s.

In contrast, the PM simultaneously learns both the flux linkages and inductances using the NN, subject to the imposed physical constraints introduced in problem (10). As shown in Fig. 3b, the d- and q-axis inductances are constrained within the ranges of $2.5 \cdot 10^{-4}$ H to $3.0 \cdot 10^{-4}$ H and $2.5 \cdot 10^{-4}$ H to $4.5 \cdot 10^{-4}$ H, respectively. The inequality constraints were active in the d-axis over the intervals $t = 0.05$ s to 0.052 s, $t = 0.252$ s to 0.353 s, and $t = 0.556$ s to 0.559 s, and in the q-axis over $t = 0.57$ s to 0.6 s, during which the corresponding Lagrange multipliers (λ_1^{in}, λ_2^{in}, and λ_3^{in}) increased. Af-

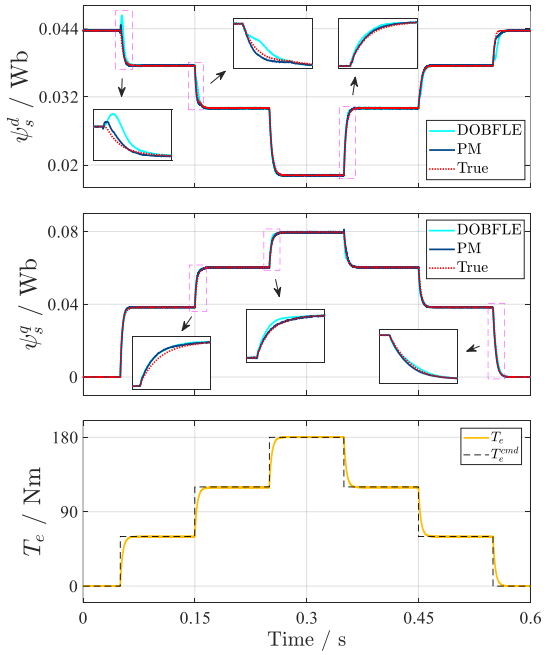

(a)

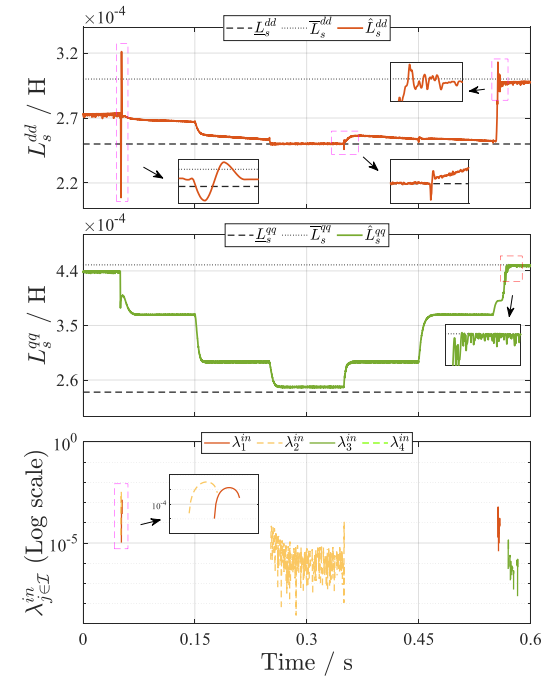

(b)

Fig. 3: Simulation results of the proposed method (PM) under a varying torque command at a speed of 500 RPM. (a) Stator flux linkage estimates from the PM and the DOBFLE in the d–q reference frame. (b) Differential inductance estimates and the corresponding Lagrange multipliers from the PM on a logarithmic scale.

ter the constraints became inactive, the Lagrange multipliers decreased and eventually converged to zero. Under these constraints, the optimization was performed according to the proposed learning rules in (13), satisfying the KKT optimality conditions, and as a result, suboptimal solutions were obtained while the flux linkages and inductances were progressively approximated. As a result, in Fig. 3a, the maximum flux linkage estimation errors in the PM are $23.66 \cdot 10^{-4}$ Wb ($\leq 5.41\%$) in the d-axis and $31.31 \cdot 10^{-4}$ Wb ($\leq 3.85\%$) in the q-axis. In comparison, the DOBFLE shows estimation errors of $53.23 \cdot 10^{-4}$ Wb ($\leq 12.19\%$) in the d-axis and $45.97 \cdot 10^{-4}$ Wb ($\leq 6.43\%$) in the q-axis.

This result demonstrates that the PM can achieve higher flux estimation accuracy than the DOBFLE, especially during transient states, by incorporating the physics of the SM, applying physical constraints on the inductances, and solving the corresponding constrained optimization problem through the weight updates of the NN.

V. Conclusion

A physics-informed online learning method for flux linkage modeling has been proposed. This method can be directly applied as a flux linkage estimator, utilizing a single-hidden-layer neural network with adaptable output layer weights. These weights are updated by minimizing the residuals of the governing PDEs while satisfying the KKT optimality conditions of a constrained optimization problem, which incorporates the physical constraints of SMs. This framework enables simultaneous learning of both flux linkages and differential inductances. The effectiveness of the proposed method was verified through simulations by comparing its flux estimation performance against that of a state-of-the-art flux estimator, DOBFLE, on a 35 kW IPMSM drive.

In future research, the NN architecture will be extended to a multi-layer structure to capture the global behavior of flux linkages using meaningful datasets collected across various operating conditions. Furthermore, the proposed approach will be validated experimentally in a laboratory environment.

References

[1] S.-K. Sul, *Control of electric machine drive systems*. John Wiley & Sons, 2011, vol. 88.

[2] C. Hackl, M. Kamper, J. Kullick, and J. Mitchell, "Current control of reluctance synchronous machines with online adjustment of the controller parameters," in *2016 IEEE 25th International Symposium on Industrial Electronics (ISIE)*, 2016, pp. 153–160, doi: 10.1109/ISIE.2016.7744882.

[3] N. Monzen and C. M. Hackl, "Optimal reference voltage saturation for nonlinear current control of synchronous machine drives," in *2024 IEEE 21st International Power Electronics and Motion Control Conference (PEMC)*, 2024, pp. 1–6, doi: 10.1109/PEMC61721.2024.10726379.

[4] K. Choi, J. Kim, and K.-B. Park, "Generalized Model Predictive Torque Control of Synchronous Machines," *IEEE/ASME Transactions on Mechatronics*, pp. 1–11, 2024, doi: 10.1109/TMECH.2024.3461209.

[5] E. Armando, R. I. Bojoi, P. Guglielmi, G. Pellegrino, and M. Pastorelli, "Experimental identification of the magnetic model of synchronous machines," *IEEE Transactions on Industry Applications*, vol. 49, no. 5, pp. 2116–2125, 2013, doi: 10.1109/TIA.2013.2258876.

[6] K. Liu, Q. Zhang, J. Chen, Z. Q. Zhu, and J. Zhang, "Online Multiparameter Estimation of Nonsalient-Pole PM Synchronous Machines With Temperature Variation Tracking," *IEEE Transactions on Industrial Electronics*, vol. 58, no. 5, pp. 1776–1788, 2011, doi: 10.1109/TIE.2010.2054055.

[7] A. Choudhury, P. Pillay, and S. S. Williamson, "Modified stator flux estimation based direct torque controlled PMSM drive for hybrid electric vehicle," in *IECON 2012-38th Annual Conference on IEEE Industrial Electronics Society*. IEEE, 2012, pp. 2965–2970, doi: 10.1109/IECON.2012.6389425.

[8] J. S. Lee, C.-H. Choi, J.-K. Seok, and R. D. Lorenz, "Deadbeat-Direct Torque and Flux Control of Interior Permanent Magnet Synchronous Machines With Discrete Time Stator Current and Stator Flux Linkage Observer," *IEEE Transactions on Industry Applications*, vol. 47, no. 4, pp. 1749–1758, 2011, doi: 10.1109/TIA.2011.2154293.

[9] A. Yoo and S.-K. Sul, "Design of Flux Observer Robust to Interior Permanent-Magnet Synchronous Motor Flux Variation," *IEEE Transactions on Industry Applications*, vol. 45, no. 5, pp. 1670–1677, 2009, doi: 10.1109/TIA.2009.2027516.

[10] N. Monzen, B. Pfeifer, and C. M. Hackl, "A simple disturbance observer for stator flux linkage estimation of nonlinear synchronous machines," in *2023 IEEE 32nd International Symposium on Industrial Electronics (ISIE)*. IEEE, 2023, pp. 1–6, doi: 10.1109/ISIE51358.2023.10227965.

[11] S. Jang, B. Pfeifer, C. M. Hackl, and K. Choi, "Extended State Observer Based Stator Flux Linkage Estimation of Nonlinear Synchronous Machines," in *2024 IEEE 33rd International Symposium on Industrial Electronics (ISIE)*. IEEE, 2024, pp. 1–5, doi:10.1109/ISIE54533.2024.10595772.

[12] S. Jang and K. Choi, "Stator Flux Linkage Estimation of Synchronous Machines Based on Integration Error Estimation for Improved Transient Performance," in *2023 62nd IEEE Conference on Decision and Control (CDC)*. IEEE, 2023, pp. 4197–4202, doi: 10.1109/CDC49753.2023.10383827.

[13] L. Ortombina, F. Tinazzi, and M. Zigliotto, "Adaptive Maximum Torque per Ampere Control of Synchronous Reluctance Motors by Radial Basis Function Networks," *IEEE Journal of Emerging and Selected Topics in Power Electronics*, vol. 7, no. 4, pp. 2531–2539, 2019, doi: 10.1109/JESTPE.2018.2858842.

[14] A. Oerder, A. Liske, and M. Hiller, "Online Identification of Nonlinear Flux Linkages Using Neural Networks for Highly Utilized PMSMs," in *2023 IEEE Energy Conversion Congress and Exposition (ECCE)*. IEEE, 2023, pp. 4959–4965, doi: 10.1109/ECCE53617.2023.10362736.

[15] J. Nocedal and S. Wright, *Numerical optimization*. Springer Science & Business Media, 2006.

[16] M. Raissi, P. Perdikaris, and G. Karniadakis, "Physics-informed neural networks: A deep learning framework for solving forward and inverse problems involving nonlinear partial differential equations," *Journal of Computational Physics*, vol. 378, pp. 686–707, 2019, doi: 10.1016/j.jcp.2018.10.045.

[17] W. Jeon, A. Chakrabarty, A. Zemouche, and R. Rajamani, "LMI-based neural observer for state and nonlinear function estimation," *International Journal of Robust and Nonlinear Control*, vol. 34, no. 10, pp. 6964–6984, 2024, doi: 10.1002/rnc.7327.

[18] S.-W. Su, C. M. Hackl, and R. Kennel, "Analytical prototype functions for flux linkage approximation in synchronous machines," *IEEE Open Journal of the Industrial Electronics Society*, vol. 3, pp. 265–282, 2022, doi: 10.1109/OJIES.2022.3162336.

[19] K. Choi, Y. Kim, K.-S. Kim, and S.-K. Kim, "Real-Time Optimal Torque Control of Interior Permanent Magnet Synchronous Motors Based on a Numerical Optimization Technique," *IEEE Transactions on Control Systems Technology*, vol. 29, no. 4, pp. 1815–1822, 2021, doi: 10.1109/TCST.2020.3006900.